Biomedical Signal Processing and Control 28 (2016) 58–62

Contents lists available at ScienceDirect

Biomedical Signal Processing and Control

journal homepage: www.elsevier.com/locate/bspc

A novel method for cardiac vector velocity measurement: Evaluation in myocardial infarction

Pablo Daniel Cruces[a,b,*], Pedro David Arini[a,b]

[a] Instituto de Ingeniería Biomédica, Facultad de Ingeniería, Universidad de Buenos Aires, Argentina
[b] Instituto Argentino de Matemática, 'Alberto P. Calderón', CONICET, Argentina

ARTICLE INFO

Article history:
Received 4 November 2015
Received in revised form 8 March 2016
Accepted 15 April 2016

Keywords:
VCG
Myocardial infarction
Cardiac vector velocity

ABSTRACT

Background and objective: Pathological alterations provoked by myocardial infarction cause slow conduction by increasing axial resistance on coupling between cells. This issue may cause abnormal patterns in the dynamics of the tip of the cardiac vector.
Methods: In this work, we have developed a method to compute the angular velocity during ventricular repolarization from Frank *XYZ* leads, using the concept of quaternion. This parameter jointly with the linear velocity obtained by differentiation and the spatial velocity reported by others during ventricular depolarization, have been combined in order to design a myocardial infarction detector (so-called index of cardiac vector velocity: ICVV) with high values of sensitivity and specificity simultaneously.
Results: The predictive power of ICVV has been tested in two groups: patients with less than 7 days after infarction, achieving 98% of sensitivity and 97% of specificity; and patients with more than 45 days after infarction, achieving 92% of sensitivity without loss of specificity. The former group is important for early detection of myocardial infarction and begins treatment in a short period of time on emergency department. The latter involves the evaluation of the cardiac vector velocity after the period of post-infarction electrical remodeling which may be useful in the follow-up of patients.
Conclusions: We have concluded that this method extends the concept of cardiac vector velocity and may be useful in the diagnosis of myocardial infarction.

1. Introduction

Early diagnosis of myocardial infarction (MI) is essential for implementing a rapid therapy to reduce possible complications or even fatal outcome. Currently, the gold standard for diagnosing a MI is a significant rise of plasma troponin levels between 12 and 24 h post myocardial injury [1]. However, this marker is elevated in a variety of other conditions and for this reason, this diagnostic criterion is supplemented with clinical judgment and several electrocardiographic (ECG) or vectorcardiographic (VCG) programs, mainly based on the presence of Q waves or changes in the ST segment [1–4]. These programs need to have high specificity to avoid unnecessarily treating patients who did not suffer a MI and high sensitivity, to quickly begin treatment of patients with early MI [5]. Unfortunately, although many modern algorithms (also including enzyme assays, body surface mapping and ECG with higher number of electrodes) might solve the first issue, it is difficult to increase sensitivity without loss of specificity [4,6,7].

Pathological alterations, provoked by fibrosis after myocardial injury, cause slow conduction by increasing axial resistance through effects on coupling between cells [8]. This fact may induce abnormal alterations in the dynamics of the cardiac vector and those alterations could be registered using the VCG which is very much utilized by physicians. Several studies have suggested the diagnostic usefulness of spatial velocity of the tip of the cardiac vector obtained during ventricular depolarization [2,9]. In the present work we have developed a novel algorithm to compute the angular and linear velocities during ventricular repolarization. We hypothesize that these parameters combined with the spatial velocity of the depolarization process can achieve high sensitivity and specificity simultaneously as discriminator of MI.

Abbreviations: AUC, area under the ROC curve; ICVV, index of cardiac vector velocity; MI, myocardial infarction; MI7, study group with MI whose VCG recording was made within the following 7 days after MI injury; MI45, study group with MI whose VCG recording was made after 45 days of injury.

* Corresponding author at: Saavedra 15, CABA C1083ACA, Argentina.
Tel.: +54 11 4954 6781x118.
E-mail address: pcruces@fi.uba.ar (P.D. Cruces).

http://dx.doi.org/10.1016/j.bspc.2016.04.003
1746-8094/

2. Materials and methods

2.1. Study population

We have used the Physikalisch-Technische Bundesanstalt (PTB) database which have been acquired at the Department of Cardiology of University Clinic Benjamin Franklin in Berlin, Germany, and has been provided to the users of PhysioNet. The data have been studied anonymously, using publicly available secondary data, therefore no ethics statement is required for this investigation [10,11]. The population consisted of 290 subjects including healthy volunteers and patients with different heart diseases. Subjects without clinical summary were excluded. Ages ranged from 17 to 87 years with a mean of 56; 81 of the subjects were female (28%). Three study groups were selected: Group 1, the control group, consisted of 52 subjects with no previous cardiovascular disease; "MI7" group, composed of 93 patients with MI with different infarct sizes and locations, whose VCG recording was made within the following 7 days after MI injury; and "MI45" group, composed of 46 patients with MI whose VCG recording was made after 45 days of MI. Each record includes 15 simultaneously measured signals: the conventional 12 leads together with the 3 Frank lead ECGs. Each signal was digitized at 1000 samples per second.

2.2. Theoretical background

This work is based on the study of the dynamics of the tip of cardiac vector, obtained from Frank leads *XYZ*. These leads define a three-dimensional space where we can describe the vector movement through two parameters: linear and angular velocities. The former quantifies the speed of linear displacement from one sample point to another one and the latter quantifies the rotation speed, i.e. the amount of time it takes to traverse an angle between two consecutive samples.

2.2.1. Linear velocity

The linear velocity in the QRS loop (so-called spatial velocity of depolarization) has been reported to be used as part of diagnostic criteria for inferior MI, but by itself it has low sensitivity [2,9]. The instantaneous values can be computed by differentiation

$$\vec{v}_i = (v_{xi}; v_{yi}; v_{zi}) = \frac{P_i(x,y,z) - P_{i+1}(x,y,z)}{Ts} \tag{1}$$

where P_i is the value of the tip of cardiac vector in *XYZ* space at *i*th sample point and *Ts* is the sampling period. Therefore, we obtain each $\vec{v}_i$ from Eq. (1) along any portion of the VCG signal path. Particularly in this work, we have evaluated not only the QRS loop (in order to obtain the classical spatial velocity), but also the linear velocity of the T-wave loop. We have proposed to characterize the resulting signal using two parameters:

- $v_{\max}$, quantifying the maximum linear speed:

$$v_{\max} = \max(|\vec{v}|) = \max(\|\vec{v}_i\|_2) \quad \forall i\text{th} \quad sample \tag{2}$$

- $v_{E\alpha}$, quantifying the total energy of the signal through the 1-norm of each α axis ($\alpha = x, y$ or z):

$$v_{E\alpha} = \|v_\alpha\|_1 = \sum_{\forall i} |v_{\alpha i}| \tag{3}$$

2.2.2. Angular velocity

Currently, in other research areas such as orbits or aerospace navigation, the rotation speed of a vector is not obtained through Euler matrices but rather through the quaternion algebra. Quaternions were first presented by Hamilton [12] over a century ago. It is well known that they play an important role in an alternative form for a rotation operator. Furthermore, quaternions are very efficient for analyzing situations which involve three dimensional rotations in terms of uncertainty propagation and data processing speed [13]. If we consider the tip of the cardiac vector as a point that rotates around the origin of the electrical axis of the heart, then we can apply the quaternion theory to compute the angular velocity.

For each pair of consecutive points P_i and P_{i+1} in *XYZ* space, normalized to the sphere of radius 1, we can define a quaternion associated with rotation angle θ:

$$\mathbf{q_i} = \cos\left(\frac{\theta}{2}\right) + \vec{u} \cdot \sin\left(\frac{\theta}{2}\right) \tag{4}$$

where the first term represents an amount of rotation and $\vec{u}$ is the rotational axis. In addition, considering the definitions of dot product and cross product

$$\begin{cases} P_i \cdot P_{i+1} = \|P_i\|_2 \cdot \|P_{i+1}\|_2 \cdot \cos(\angle(P_i, P_{i+1})) \\ P_i \times P_{i+1} = \|P_i\|_2 \cdot \|P_{i+1}\|_2 \cdot \sin(\angle(P_i, P_{i+1})) \cdot \vec{n} \end{cases} \tag{5}$$

we obtain

$$\mathbf{q_i} = (P_i \cdot P_{i+1}; P_i \times P_{i+1}) \tag{6}$$

which computes the quaternion for double-angle value.

Once each quaternion that describes rotation from P_i to P_{i+1} was obtained, the instantaneous angular velocity can be computed by solving the Poisson equation [14]:

$$\dot{\mathbf{q}}_\mathbf{i} = \frac{1}{2} . \vec{w}_i . \mathbf{q_i} \tag{7}$$

Finally, multiplying both sides by the inverse of the quaternion and bearing in mind that we obtained a double-angle expression, then

$$\vec{w}_i = \dot{\mathbf{q}}_\mathbf{i} . \mathbf{q_i}^{-1} \tag{8}$$

As in Section 2.2.1, we obtain several descriptors for the angular velocity along the T-wave loop on the VCG signal path:

- $w_{\max}$, quantifying the maximum angular speed:

$$w_{\max} = \max(|\vec{w}|) = \max(\|\vec{w}_i\|_2) \quad \forall i\text{th} \quad sample \tag{9}$$

- $w_{E\alpha}$, quantifying the total energy of the signal through the 1-norm of each α axis ($\alpha = x, y$ or z):

$$w_{E\alpha} = \|w_\alpha\|_1 = \sum_{\forall i} |w_{\alpha i}| \tag{10}$$

2.3. Algorithm

The *XYZ* signals were selected for each recording. A Butterworth high-pass filter (0.5 Hz, bidirectional) has been applied for baseline wander correction. We have defined two signal windows: The first in R-wave peak position ±60 ms and the second in T-wave peak position ±120 ms. In order to reduce high frequency noise in both signals, a Butterworth bidirectional low-pass filter (45 Hz and 20 Hz, respectively) has been used. QRS complexes and T-waves have been located using the wavelet-transform based method in [15].

Given that tissue damage constantly alters the conduction velocity in every beat [8] and that our hypothesis is based on the fact that these alterations may be measured from the VCG, we have calculated the velocity signals of Sections 2.2.1 and 2.2.2 on each beat and subsequently applied an average on 50 beats. For this purpose, it has performed an alignment of each signal based on minimizing the mean square error.

We have shown in Fig. 1 an example of $\vec{v}_i$ and $\vec{w}_i$ signals resulting from the algorithm in a scaled T-wave loop.

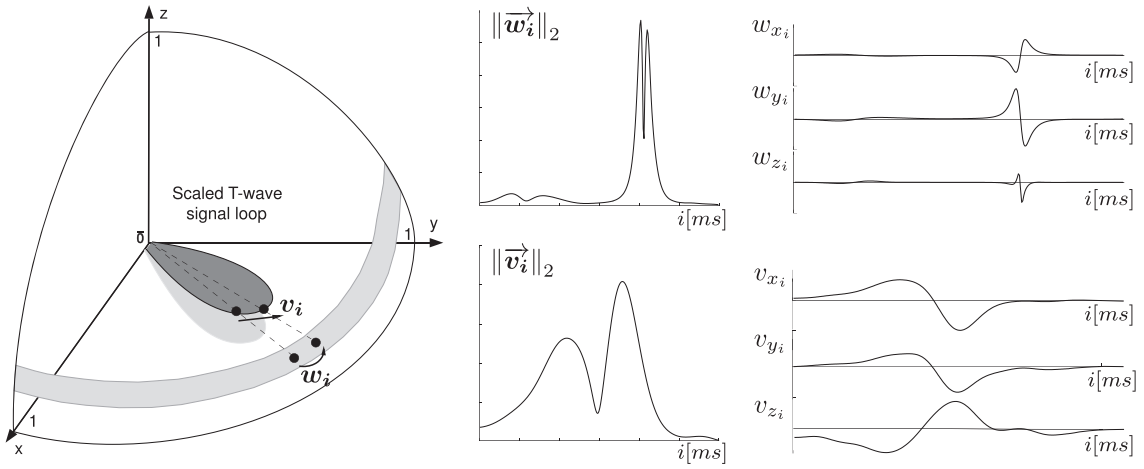

Fig. 1. Example of angular and linear velocities of the tip of the cardiac vector in a 3D graph (left panel) of a T-wave loop. Using the 2-norm graph (middle panel) we obtain the maximum speeds of the loop. From each velocity in a given axis (right panel) we obtain the total energy applying the 1-norm.

Table 1
Mean values and standard deviations of parameters that showed the greatest significant differences between control and MI groups. (QRS) indicates that the parameter was obtained from QRS-complex and (T) from T-wave.

Parameter	Group	No. of subjects	Mean	Standard deviation	p-Value
	Control	52	18.6 μV/ms	7.5 μV/ms	–
$v_{\max}$ (T)	MI7	93	8.4 μV/ms	3.1 μV/ms	$<10^{-12}$
	MI45	46	8.9 μV/ms	5.1 μV/ms	$<10^{-7}$
	Control	52	0.3 rad/ms	0.2 rad/ms	–
w_{Ey} (T)	MI7	93	0.1 rad/ms	0.1 rad/ms	$<10^{-12}$
	MI45	46	0.1 rad/ms	0.1 rad/ms	$<10^{-6}$
	Control	52	251.5 μV/ms	78.9 μV/ms	–
$v_{\max}$ (QRS)	MI7	93	141.5 μV/ms	49.9 μV/ms	$<10^{-13}$
	MI45	46	134.2 μV/ms	34.4 μV/ms	$<10^{-11}$

2.4. Statistical analysis

Using a two-sided Wilcoxon signed rank test, we have determined the parameters with statistically significant differences ($p < 0.05$) between control and the different MI groups. In order to find the maximum pair of specificity/sensitivity, those parameters that have been statistically significant are used for calculating a unique descriptor (which we have called index of cardiac vector velocity: ICVV) through a linear discriminant analysis.

Receiver operator characteristic (ROC) curves have been computed for ICVV descriptor. In order to evaluate its predictive power, we have reported the area under the ROC curve (AUC) as well as both specificity and sensitivity in optimal level. Likewise, it is also obtained for the same decision criterion, the probability of success in detecting MI patients with a positive test (positive predictive value: PPV) and the probability of a negative test when the subject is healthy (negative predictive value: NPV).

3. Results

Table 1 gives the mean and standard deviation of the parameters with the smallest p-values and the amount of subjects in each group. As it can be seen, the greatest differences between healthy subjects and MI patients have been observed in the $v_{\max}$ (QRS) parameter. However, $v_{\max}$ (QRS) alone has levels of specificity and sensitivity (close to 90%) equivalents to that of MI discriminators on the state-of-the-art. On the other hand, the p-values are lower in the "MI45" group that refer to recordings made after 45 days from MI.

Then, we have computed a weighted combination of the w_{Ey} (T), $v_{\max}$ (T) and $v_{\max}$ (QRS). We have chosen a proper weight for each parameter in order to get a value of the same order of magnitude when multiplying each one by the indicated weight:

$$\mathrm{ICVV} = 100 \cdot w_{\mathrm{Ey}}\ (\mathrm{T}) + 10 \cdot v_{\max}\ (\mathrm{T}) + 1 \cdot v_{\max}\ (\mathrm{QRS}) \tag{11}$$

The ICVV descriptor obtained from Eq. (11), reaches a significance value less than 10^{-20}. Table 2 shows the values of PPV, NPV, sensitivity and specificity for each MI group. The decision criterion is included in the table. Both for patients with recent MI as those with more than a month and a half since the injury, the index achieved an extremely high AUC.

4. Discussion

With the aim of efficiently detecting a MI through a non-invasive method, a new outlook to analyze the VCG has been introduced

Table 2
Evaluation of predictive power of ICVV descriptor.

Group	Mean	Standard deviation	PPV	NPV	Sensitivity	Specificity	Criterion	AUC
Control	467.0	143.1	–	–	–	–	–	–
MI7	236.0	59.4	98	97	98	97	<318	99
MI45	235.8	67.8	96	93	92	97	<316	98

through the study of the velocities of the tip of cardiac vector. The choice of VCG instead of the ECG is appropriate considering that several works have shown its efficiency in studying the effects of MI [16–18]. Additionally, in order to evaluate the velocity dynamics of the cardiac vector in both the early stage of MI and after the electrical remodeling phenomenon which often occurs over several weeks post-MI [19,20], we have assessed separately the recordings of the first 7 days since myocardial injury from the recordings acquired after 45 days.

For both linear and angular velocities, it has been found significant differences in the T-wave and in the QRS-complex (see Table 1). This verifies our hypothesis in which we assumed that these velocities, obtained from VCG, would be affected by the effect of fibrosis after MI. Moreover, it may be observed that MI patients have smaller mean values that may be associated with an impairment of the conduction paths caused by the increase of axial resistance on coupling between cells.

Several of published criteria for MI diagnosis are based on the presence of Q waves (broad and deep negative deflections). However, Q waves may not be evident in many cases of inferior or lateral MI and are often missed, reducing specificity [1,2,21,22]. Moreover, in the follow-up of patients there is usually a significant sensitivity reduction in detecting prior infarctions [23]. Recent studies have sought to overcome this problem by other methods than Q-waves through the computation of ECG morphological abnormalities in the dispersion of depolarization and repolarization [24,25]. Moreover, it has been shown that abnormal changes in the amplitude of the T wave in the precordial leads are able to detect prior lateral MI with a sensitivity/specificity of 44%/80% [24]. Other works have achieved better sensitivity values by analyzing changes in the ST-T segment in the 12-lead ECG in the earliest manifestations of MI [26]. Also, it has been observed that the addition of the posterior leads (V7, V8 and V9) improves the predictive power of ST-T markers when injury occurs in the inferior wall of the myocardium [27]. Nevertheless, despite this improvement in sensitivity through the study of ST-segment changes, these methods have poor specificity since such alterations appear in many other conditions [26]. In addition, few hours after injury, ischemic myocardium becomes necrotic and in many cases, it can be seen a normalization (un retorno al nivel isoelectrico normal) of the ST segment [28]. Some authors have reported values sensitivity and specificity close to 90% for diagnosing MI obtained by other methods (i.e. when the diagnosis is made through body surface mapping method [4], with modern techniques with higher number of ECG electrodes [6,29], or is made by an expert cardiologist [30]). The study of blood troponin levels may lead to a raised sensitivity but it requires to be carried out between 12 and 24 h following myocardial injury. Before or after that time period, the study shows poor results [1].

On the other hand, we have applied the quaternions theory in order to furnish a mathematical method for representing orientation and rotation of the tip of the cardiac electrical vector in 3D. From the point of view of computational calculation the quaternions theory has shown several advantages, mainly related to the quaternion product which allows a simpler composition compared with the Euler angles. Moreover, the quaternions are more efficient and stable numerically in contrast with the rotation matrices [13].

Through the ICVV descriptor, obtained from Eq. (11), we have achieved very high values of sensitivity (98%) and specificity (97%) in those recordings of less than 7 days (see Table 2). In addition, for those records over 45 days, we have achieved a (92%) of sensitivity with no loss of specificity (97%). While it could be assumed that the reason of this reduction is due to electrical remodeling effects, it should be noted that the amount of patients in both groups is quite different. In any case, the ICVV descriptor shows a very high potential for discriminating control subjects from MI patients since it has reached an AUC value of 99% in the MI7 group and of 98% in the MI45 group.

5. Study limitations

The parameters that have been presented in this work have low dependence on the accuracy of the time-domain interval measurements. This suggests that they are highly reproducible. However, further investigations are needed to test the reproducibility with other VCG databases.

6. Conclusions

We have introduced a new method which is able to quantify the instantaneous values of the angular velocity of the tip of cardiac vector in the *XYZ* space using the concept of quaternion. We have proved that this parameter is affected by a MI as well as the linear velocity. Consequently, the ICVV descriptor, computed through a linear combination of these parameters, is able to differentiate the healthy subjects from MI patients, reaching a very high value of sensitivity without loss of specificity in both early and late stages of infarction. This method extends the concept of cardiac vector velocity and may be useful in the diagnosis of myocardial infarction.

Conflicts of interest

The authors declare that there are no conflicts of interest.

Acknowledgement

This work was supported by CONICET, under project PIP #538, Agencia Nacional de Promoción Científica y Tecnológica, Argentina.

Appendix A. Poisson equation

First of all, let us suppose we have two consecutive points of the tip of cardiac vector in *XYZ* space separated a certain amount of time Δt, i.e. $\mathbf{q}(t)$ and $\mathbf{q}(t+\Delta t)$. In order to study the dynamics of the rotation we can define the derivative of the quaternion through its definition:

$$\dot{\mathbf{q}}(t) = \lim_{\Delta t \to 0} \frac{\mathbf{q}(t+\Delta t) - \mathbf{q}(t)}{\Delta t} \tag{A.1}$$

Taking advantage of the quaternion product we can write $\mathbf{q}(t+\Delta t)$ as a composition of rotations

$$\mathbf{q}(t+\Delta t) = \mathbf{q}(\Delta t) \cdot \mathbf{q}(t) \tag{A.2}$$

The quaternion $\mathbf{q}(\Delta t)$ can be written using the angular velocity and the trigonometric form.

$$\mathbf{q}(\Delta t) = \cos\left(\frac{\omega \Delta t}{2}\right) + \vec{u} \cdot \sin\left(\frac{\omega \Delta t}{2}\right) \approx 1 + \vec{u}\frac{\omega}{2}\Delta t + o(\Delta t) \tag{A.3}$$

where $\vec{u}$ is the rotational axis. Since sine and cosine are given in terms of the trigonometric series, then $o(\Delta t)$ is an infinite polynomial: $o(\Delta t) = k1(\Delta t)^2 + k2(\Delta t)^3 + \cdots$. Combining equations, we have

$$\begin{aligned} \mathbf{q}(t+\Delta t) &= \left(1 + \vec{u}\frac{\omega}{2}\Delta t + o(\Delta t)\right) \cdot \mathbf{q}(t) \\ &= \mathbf{q}(t) + \frac{\vec{\omega}.\mathbf{q}(t)}{2}\Delta t + o(\Delta t) \cdot \mathbf{q}(t) \end{aligned} \tag{A.4}$$

Rearranging terms and dividing by Δt we get

$$\frac{\mathbf{q}(t+\Delta t) - \mathbf{q}(t)}{\Delta t} = \frac{\vec{\omega} \cdot \mathbf{q}(t)}{2} + \frac{o(\Delta t) \cdot \mathbf{q}(t)}{\Delta t} \tag{A.5}$$

Finally, taking limit $\Delta t \to 0$

$$\dot{\mathbf{q}}(t) = \frac{\vec{\omega} \cdot \mathbf{q}(t)}{2} \tag{A.6}$$

which leads to the Poisson equation for the instantaneous double-angle. Since the *XYZ* records are sampled signals of the continuous loop, we can solve Eq. (A.6) using difference equations taking into account the sampling period *Ts*. Expressing the inverse of the quaternion in terms of its conjugate and its norm, we can compute the instantaneous angular velocity as follows

$$\vec{w}_i = \dot{\mathbf{q}}_\mathbf{i} \cdot \mathbf{q}_\mathbf{i}^{-1} = \left(\frac{\mathbf{q}_{i+1} - \mathbf{q}_\mathbf{i}}{Ts} \right) \cdot \frac{\overline{\mathbf{q}_\mathbf{i}}}{\left\| \mathbf{q}_\mathbf{i} \right\|} \tag{A.7}$$

References

[1] N. Herring, D. Paterson, ECG diagnosis of acute ischaemia and infarction: past, present and future, Q. J. Med. 99 (2006) 219–230.
[2] R. Warner, N. Hill, I. Rowlandson, S. Mookherjee, H. Smulyan, Importance of the distance and velocity of electrical forces in the diagnosis of inferior wall healed myocardial infarction: a vectorcardiographic study, Am. J. Cardiol. 57 (1986) 725–728.
[3] C. Lefebvre, J. Hoekstra, Early detection and diagnosis of acute myocardial infarction: the potential for improved care with next-generation, user-friendly electrocardiographic body surface mapping, Am. J. Emerg. Med. 25 (2007) 1063–1072.
[4] J. Hoekstra, B. O'Neill, Y. Pride, C. Lefebvre, D. Diercks, W. Peacock, G. Fermann, C. Gibson, D. Pinto, J. Giglio, A. Chandra, C. Cairns, M. Konstam, J. Massaro, M. Krucoff, Acute detection of ST-elevation myocardial infarction missed on standard 12-lead ECG with a novel 80-lead real-time digital body surface map: primary results from the multicenter OCCULT MI trial, Ann. Emerg. Med. 54 (6) (2009) 780–788.
[5] P. Elko, W. Weaver, P. Kudenchuk, The dilemma of sensitivity versus specificity in computer-interpreted acute myocardial infarction, J. Electrocardiol. 24 (1992) 2–7.
[6] M. Weil, M. Oehler, M. Schilling, L. Maier, First clinical evaluation of a novel capacitive ECG system in patients with acute myocardial infarction, Clin. Res. Cardiol. 101 (2012) 165–174.
[7] Z. Zhelev, C. Hyde, E. Youngman, M. Rogers, S. Fleming, T. Slade, H. Coelho, T. Jones-Hughes, V. Nikolaou, Diagnostic accuracy of single baseline measurement of Elecsys Troponin T high-sensitive assay for diagnosis of acute myocardial infarction in emergency department: systematic review and meta-analysis, Br. Med. J. 350 (2015) 1–14.
[8] P. Macfarlane, A. Van Oosterom, O. Pahlm, P. Kligfield, M. Janse, J. Camm (Eds.), Comprehensive Electrocardiology, vol. 3, Springer, 2011, pp. 1108–1112 (Chapter 23).
[9] Y. Sakamoto, S. Kokusho, T. Hiroki, T. Sano, Depolarization phase of the spatial velocity electrocardiogram in normal and ventricular overloading, J. Electrocardiol. 6 (1) (1973) 19–26.
[10] R. Bousseljot, D. Kreiseler, A. Schnabel, Nutzung der ekg-signaldatenbank cardiodat der ptb über das internet, Biomedizinische Technik 1 (1995) 317.
[11] A. Goldberger, L. Amaral, L. Glass, H. J.M., I. P.C., R. Mark, M. J.E., G. Moody, C.-K. Peng, H. Stanley, Physiobank, physiotoolkit, and physionet: components of a new research resource for complex physiologic signals, Circulation 101 (23) (2000) e215–e220.
[12] S. Mathematica (Ed.), A Collection of Papers in Memory of Sir William Rowan Hamilton, Scripta Mathematica Studies, 1945, pp. 37–49 (Chapter 5).
[13] J. Kuipers, Quaternions and Rotation Sequences: A Primer with Applications to Orbits, Aerospace and Virtual Reality, Princeton University Press, 1999, pp. 103–139 (Chapter 5).
[14] A. Poznyak, Modelado Matemático de los Sistemas Mecánicos, Electricos y Electromecánicos, Pearson, 2005, pp. 73–83 (Chapter 2).
[15] J. Mendieta, Algoritmo para el delineado de se nales electrocardiográficas en un modelo animal empleando técnicas avanzadas de procesamiento de se nales, Electrical Engineering Thesis, Facultad de Ingeniería de la Universidad de Buenos Aires, 2012.
[16] J. Starr, G. Wagner, R. Draffin, J. Reed, A. Walaton II, V. Sehar, Vectorcardiographic criteria for the diagnosis of anterior myocardial infarction, Circulation 53 (1976) 229–234.
[17] H. Hurd II, M. Starling, M. Crawford, P. Dlabal, R. O'Rourke, Comparative accuracy of electrocardiographic and vectorcardiographic criteria for inferior myocardial infarction, Circulation 63 (5) (1981) 1025–1029.
[18] M. Hasan, D. Abbott, M. Baumert, Beat-to-beat vectorcardiographic analysis of ventricular depolarization and repolarization in myocardial infarction, PLoS ONE 7 (11) (2012) 1–10.
[19] J. Pinto, P. Boyden, Electrical remodeling in ischemia and infarction, Cardiovasc. Res. 42 (1999) 284–297.
[20] M. Cutler, D. Jeyaraj, D. Rosenbaum, Cardiac electrical remodeling in health and disease, Trends Pharmacol. Sci. 32 (3) (2011) 174–180.
[21] O. Pahlm, D. Case, G. Howard, J. Pope, W. Haisty, Decision rules for the ECG diagnosis of inferior myocardial infarction, Comp. Biomed. Res. 23 (1990) 332–345.
[22] P. Elko, I. Rowlandson, A statistical analysis of the ECG measurements used in computerized interpretation of acute anterior myocardial infarction with applications to interpretive criteria development, J. Electrocardiol. 25 (1992) 113–119.
[23] F. Asch, C.S. Shah, S. Rattin, A. Swaminathan, L.J. Fuisz, Lack of sensitivity of the electrocardiogram for detection of old myocardial infarction: a cardiac magnetic resonance imaging study, Am. Heart J. 152 (4) (2006) 742–748.
[24] D. Rovai, A. Gimelli, M. Coceani, F. Sbrana, G. Masini, G. Rossi, T wave abnormalities identify patients with previous lateral wall myocardial infarction and circumflex artery disease, J. Electrocardiol. 49 (2) (2015) 216–222.
[25] S. Recke, Non-Q-wave-electrocardiograms. Signs of earlier myocardial infarction, Med. Klin. Intensivmed. Notfmed. 107 (8) (2012) 634–640.
[26] G. Coppola, P. Carità, E. Corrado, A. Borrelli, A. Rotolo, M. Guglielmo, C. Nugara, L. Ajello, M. Santomauro, S. Novo, ST segment elevations: always a marker of acute myocardial infarction? Indian Heart J. 65 (4) (2013) 412–423.
[27] D. Pradhan, S. Jian, R. Shrestha, M. Gupta, S. Karki, F.L.X.S. Rajbhandari, Clinical significance of ST segment elevation in posterior leads V7, V8 and V9 in patients with acute inferior wall myocardial infarction, J. Cardiovasc. Dis. Diagn. 1 (2) (2013) 1–5.
[28] F. Vervaat, S. Bouwmeester, I. Van Hellemond, G. Wagner, A. Gorgels, Consideration of QRS complex in addition to ST-segment abnormalities in the estimation of the "risk region" during acute anterior or inferior, J. Electrocardiol. 47 (4) (2014) 535–539.
[29] E. Trägårdh, M. Claesson, G. Wagner, S. Zhou, O. Pahlm, Detection of acute myocardial infarction using the 12-lead ECG plus inverted leads versus the 16-lead ECG (with additional posterior and right-sided chest electrodes), Clin. Physiol. Funct. Imaging 27 (2007) 368–374.
[30] I. Rowlandson, P. Kudenchuk, P. Elko, Computerized recognition of acute infarction: criteria advances and test results, J. Electrocardiol. 23 (1990) 1–5.